

Chameleon: a Heterogeneous and Disaggregated Accelerator System for Retrieval-Augmented Language Models

Wenqi Jiang¹, Marco Zeller¹, Roger Waleffe², Torsten Hoefler¹, and Gustavo Alonso¹

¹Department of Computer Science, ETH Zurich

²Department of Computer Science, University of Wisconsin-Madison

Abstract

A Retrieval-Augmented Language Model (RALM) augments a large language model (LLM) by retrieving context-specific knowledge from an external database via vector search. This strategy facilitates impressive text generation quality even with smaller models, thus reducing computational demands by orders of magnitude. However, RALMs introduce unique system design challenges due to (a) the diverse workload characteristics between LLM inference and retrieval and (b) the various system requirements and bottlenecks for different RALM configurations such as model sizes, database sizes, and retrieval frequencies. We propose *Chameleon*, a heterogeneous accelerator system that integrates both LLM and retrieval accelerators in a disaggregated architecture. The heterogeneity ensures efficient acceleration of both LLM inference and retrieval, while the disaggregation allows independent scaling of LLM and retrieval of accelerators to fulfill diverse RALM requirements. Our Chameleon prototype implements retrieval accelerators on FPGAs and assigns LLM inference to GPUs, with a CPU server orchestrating these accelerators over the network. Compared to CPU-based and CPU-GPU vector search systems, Chameleon’s retrieval accelerators achieve up to $23.72\times$ speedup and $26.2\times$ energy efficiency. Evaluated on various RALMs, Chameleon exhibits up to $2.16\times$ reduction in latency and $3.18\times$ speedup in throughput compared to the hybrid CPU-GPU architecture. These promising results pave the way for bringing accelerator heterogeneity and disaggregation into future RALM systems.

1 Introduction

The recent advances in generative large language models (LLMs) are attributable to the surging scale of transformer neural networks. These models, trained on massive datasets, often encompass hundreds of billions of parameters [10, 19, 84, 95]. The intuition behind the scaling-up approach is to leverage more model parameters to learn and encapsulate

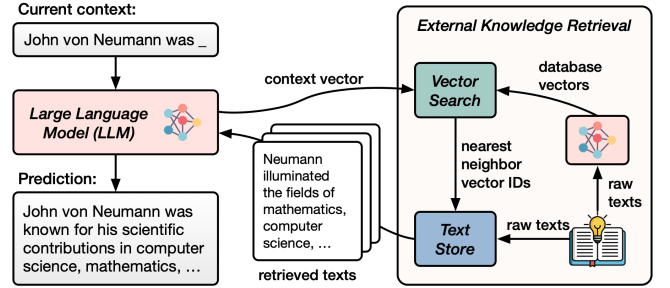


Figure 1: Retrieval-augmented language model (RALM) architecture.

textual knowledge, thus offering more precise and informed responses.

However, improving LLM quality by expanding model sizes leads to three major problems. Firstly, the increased computational demands result in higher inference costs [7, 10]. Secondly, updating knowledge in the LLM is inflexible: the latest information, like recent news, is not incorporated without additional training, and removing harmful or sensitive data, such as personal information mistakenly included in the training set [11, 100], can be difficult, often requiring the model to be retrained from scratch [9, 12]. Finally, the trustworthiness of such models is still a matter of concern. An LLM can produce non-factual content [68, 71] because it is challenging to ascertain if the model has acquired the specific knowledge pertinent to the context, and even if it has, there is no guarantee it will employ that knowledge during text generation.

One effective approach to address the aforementioned problems is known as *Retrieval-Augmented Language Models (RALMs)*: the LLM focuses on learning linguistic structures, while context-specific knowledge is incorporated during inference. Figure 1 overviews the RALM architecture. The external knowledge database encodes textual knowledge into

vectors using LLMs and stores them in a vector database. During inference, the knowledge retriever identifies relevant knowledge in the database via vector search, which assesses relevance by computing the similarity between the context vector and the database vectors. Since knowledge is primarily retrieved rather than encoded in the LLM’s parameters, RALMs, even with LLMs of one to two orders of magnitude fewer parameters, can achieve superior or comparable performance to conventional LLMs on various natural language processing (NLP) tasks, including question answering [8, 42, 43, 68, 89], dialogue systems [58, 93], language modeling [33, 57, 104], and machine translation [56, 67], thus significantly lowering the compute costs during inference. Additionally, knowledge editing can be achieved by simply updating the database, without retraining the LLM. Moreover, RALMs can produce tailored sequences by accessing, e.g., a personal email database, circumventing the inclusion of private data into the LLM’s training corpus and consequently diminishing privacy concerns.

Despite its advantages, efficient RALM inference presents two challenges. *First*, the workload characteristics of the LLM and the retriever are distinct. While the LLM inference primarily relies on rapid matrix multiplication, the retrieval system — often utilizing fast search algorithms like Product Quantization (PQ) [46] — demands both substantial memory capacity for the vector database and fast processing of quantized database vectors during query time. Unfortunately, neither GPUs nor CPUs are perfect for large-scale vector search. The memory capacity requirement hampers the deployment of retrievers on GPU clusters, as it can be cost-prohibitive given the limited device memory capacity per GPU. On the other hand, transferring the database vectors from the host server to the GPU at query time severely compromises performance, given the low data movement bandwidth relative to the GPU’s device memory. Although CPUs can be coupled with abundant DRAM, they are too slow in evaluating distances between query vectors and quantized database vectors, given the many per-PQ-code cache accesses and instruction dependencies that occur during a search. *Second*, the diverse range of RALM configurations leads to shifting system requirements and bottlenecks. Various model sizes, database sizes, and retrieval frequencies can be used in a RALM, each introducing unique requirements for LLM inference performance, retrieval performance, and memory capacity for the vector database.

We envision a high-performance and efficient RALM system to adhere to two key design principles. According to Amdahl’s law, performance gains achieved by accelerating one of the RALM components, whether LLM inference or vector search, are limited by the proportion of execution time of that component. Thus, the first design principle we propose is to incorporate *heterogeneous accelerators* tailored for both RALM components rather than only employing inference accelerators such as GPUs. Secondly, the heterogeneous accel-

erators should be *disaggregated* to support diverse RALM demands efficiently, in contrast to a monolithic approach where a fixed number of LLM and retrieval accelerators reside on the same server. The rationale is twofold: (a) performance bottlenecks vary between different RALMs, with some demanding frequent retrieval from large databases, while others are mainly limited by the LLM inference performance, thus requiring a model-specific optimal balance between the two types of accelerators; and (b) a huge vector database may necessitate more retrieval accelerators than a single server can accommodate.

To materialize this vision, we propose *Chameleon*, a heterogeneous and disaggregated accelerator system for efficient, flexible, and high-performance RALM inference. Chameleon consists of three primary components. Firstly, *ChamVS* is a distributed and accelerated vector search engine. It consists of several disaggregated memory nodes, each containing a shard of quantized database vectors in DRAM, a near-memory retrieval accelerator prototyped on an FPGA, and a hardware TCP/IP stack. Secondly, *ChamLM* is a multi-GPU LLM inference engine. It produces query vectors and generates texts using the retrieved information. Lastly, a CPU coordinator server orchestrates the network communication between the retrieval and LLM accelerators and converts the retrieved vector IDs into their respective textual representations.

We evaluate Chameleon with different LLM architectures, LLM sizes, database sizes, and retrieval frequencies. For large-scale vector search, ChamVS achieves up to $23.72\times$ latency reduction compared to the state-of-the-art CPU-based vector search system while consuming $5.8\sim 26.2\times$ less energy per query. For end-to-end RALM inference, Chameleon achieves up to $2.16\times$ speedup in latency and $3.18\times$ increase in throughput compared to the hybrid CPU-GPU architecture. We further illustrate that the optimal balance between the two types of accelerators varies significantly across different RALMs, making disaggregation essential for achieving both flexibility and high accelerator utilization rates. The impressive performance and flexibility of Chameleon encourage future RALM systems to adopt such a heterogeneous and disaggregated design.

Contributions:

- We propose Chameleon, a disaggregated system consisting of heterogeneous hardware for efficient RALM inference.
- We design and implement ChamVS, a distributed engine for large-scale vector search, which includes:
 - Accelerated disaggregated memory nodes, each equipped with a specialized near-memory vector search processor.
 - A novel hardware design for fast top-K selection while consuming minimal hardware resources.

- A GPU-based vector index scanner to prune search space.
- We build ChamLM, a multi-GPU engine for producing queries and generating texts using retrieved knowledge.
- We evaluate Chameleon using various RALM configurations and showcase its remarkable performance and efficiency.

2 Background and Motivation

2.1 Retrieval-Augmented Language Models

A RALM combines a transformer-based LLM [22, 83, 85] with an external knowledge database. During inference, information relevant to the current context is retrieved from the database and utilized by the LLM to predict subsequent tokens. We classify RALMs by the content they retrieve:

The first category of RALMs retrieves *text chunks* containing multiple tokens related to the current context. Popular examples of this category employ the *encoder-decoder* transformer architecture [8, 42, 68], as the decoder-only models are less flexible in integrating text chunks [86]. The encoder-decoder model comprises two primary components: an encoder, responsible for processing retrieved texts, and a decoder, which produces output tokens. During inference, initial states, such as a user’s prompt, are vectorized to retrieve context-related knowledge, i.e., text chunks in the database with similar vector representations [8, 43, 68]. The retrieved text chunks are then concatenated and processed by the encoder, and their latent knowledge representations are conveyed to the decoder via the cross-attention mechanism [97], leading to the generation of output tokens. When generating long sequences, however, the generated content may gradually diverge from the initially retrieved contents. Thus, instead of initiating retrieval only once at the beginning [42, 68, 89], an effective strategy is to perform multiple retrievals during text generation to improve token generation quality [86], for instance, at a regular interval of every 64 generated tokens [8].

The second category of RALMs retrieves only the *next token* of each similar context in the database. These RALMs employ a *decoder-only* model [4, 57, 76]. At each step of token generation (retrieval interval is one), the last layer’s hidden state serves as the query to retrieve similar contexts and the next token of each similar context [57, 76, 103]. The next token of the current context is then predicted by interpolating the next-token probability distribution predicted by the model with that of the retrieved content [56, 57].

From a system performance standpoint, the two categories differ in two aspects. Firstly, regarding the retrieval interval, the latter category retrieves every step during token generation (higher retrieval cost), while the former category may either employ multiple-token intervals or retrieve just once at the beginning per sequence. Secondly, in terms of computation

Table 1: Definitions of important symbols in IVF-PQ.

Symbol	Definition
x	A query vector.
y	A database vector.
m	The sub-space number of product quantization.
$nlist$	The number of clusters in the IVF index.
$nprobe$	The number of IVF lists to scan per query.
K	The number of nearest neighbors to return.

cost, the former category, which often adopts the encoder-decoder architecture, introduces the cost of encoder inference per retrieval step and cross-attentions between decoder and encoder every token generation step (higher computational cost), while the latter category, with a decoder model, only requires an extra interpolation of the next token’s probability distribution, introducing minimal computational overhead.

2.2 Large-Scale Vector Search

A vector search takes a D -dimensional query vector x as input and retrieves K relevant vector(s) from a database Y , populated with many D -dimensional vectors, based on similarity metrics like L2 distances. While the nearest neighbor search retrieves the exact K closest vectors, linearly scanning through a large vector set can be prohibitively expensive. Thus, real-world vector search systems adopt approximate nearest neighbor (ANN) search that trades accuracy for much higher system performance. The quality of an ANN search is measured by the recall at K ($R@K$), which denotes the overlap percentage between the exact K nearest neighbors and the K returned by the ANN. In the subsequent sections, we will use the terms *vector search* and *ANN search* interchangeably.

IVF-PQ is currently the most popular vector search algorithm in RALMs [8, 42, 57, 68] thanks to its great performance in large-scale ANN search [31, 46, 51]. IVF-PQ combines (a) an inverted-file (IVF) index to prune the search space and (b) product quantization (PQ) to compress database vectors and reduce the computational demands during the search process. The parameters in IVF-PQ are shown in Table 1.

Inverted-File (IVF) Index. An IVF index divides a vector dataset Y into many ($nlist$) disjoint subsets, typically using clustering algorithms like K-means. Each of these subsets is termed an IVF list. At query time, the IVF index is scanned, and only a select few ($nprobe$) IVF lists whose cluster centroids are close to the query vector are scanned, such that the search space is effectively pruned.

Product Quantization (PQ). PQ reduces memory usage and computational requirements of vector search by compressing each database vector into m -byte PQ codes. The training and searching workflow of PQ is shown in Figure 2.

To quantize database vectors, all database vectors are partitioned evenly into m sub-vectors ①. Each sub-vector pos-

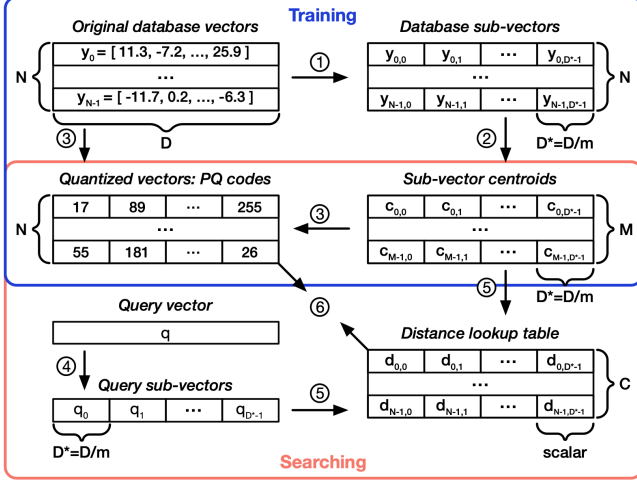


Figure 2: Product quantization (PQ) in training and searching.

sesses a dimensionality of $D^* = \frac{D}{m}$, typically ranging from 4 to 16 in practice. A clustering algorithm is performed in each sub-space ② and results in a list of centroids c , allowing each database sub-vector to be approximated by its nearest centroid. Typically, the number of clusters per sub-space is set as $M = 256$, such that a cluster ID can be represented with one byte. Consequently, once the cluster centroids are stored, each database vector can be represented by m -byte PQ codes.

During the search process, a query vector will be compared against the quantized database vectors. The distance computation can be formulated as $\hat{d}(x, y) = d(x, c(y)) = \sum_{i=1}^m d(x_i, c_i(y_i))$, where $\hat{d}(x, y)$ is the approximate distance between a query vector x and a quantized database vector y , and $c(y)$ is the reconstructed database vector using the PQ codes and the cluster centroid vectors per sub-space. To calculate $\hat{d}(x, y)$, the query vector is divided into m sub-vectors (x_i) ④ and compared against the reconstructed quantized sub-database-vectors $c_i(y_i)$. To speed up distance computations with many database vectors, it would be beneficial to construct a distance lookup table ⑤ that can be reused within a query, encompassing all combinations between a sub-query-vector and a cluster centroid within the same sub-space. With this table, the value of $d(x_i, c_i(y_i))$ can be swiftly retrieved by a table lookup operation, utilizing the PQ code as the address ⑥, leading to improved computational efficiency.

2.3 Motivation: Efficient RALM Inference

An efficient RALM inference engine should meet the following **system requirements**:

- Both the LLM inference and the large-scale vector search components should be fast and resource-efficient.
- The system should be flexible enough to accommodate diverse RALM configurations, spanning various combi-

nations of (a) transformer architectures, (b) model sizes, (c) database sizes, and (d) retrieval frequencies.

However, little effort has been devoted to developing efficient RALM systems that meet the above requirements. This is likely because RALM has been an emerging topic within the machine learning community. Specifically, the current RALM systems employed in machine learning research [8, 42, 43, 57, 68] exhibit the following shortcomings:

First, each research RALM system focuses on *being able to run* one or a small number of RALM models, paying little attention to performance, resource efficiency, and system adaptability for diverse RALM configurations.

Second, while hardware accelerators for LLMs, such as GPUs, are advancing rapidly, less attention has been paid to the retrieval aspect, which, as our evaluations will demonstrate, can become the performance bottleneck in RALM inference because neither CPUs nor GPUs are the ideal processors to search on such a vast volume of vector data.

On the one hand, CPUs are slow in scanning PQ codes during query time ⑥. This inefficiency arises due to the frequent cache accesses (for each byte of PQ code, load the code and use it as an address to load a distance) and the instruction dependencies between operations (distance lookups depend on PQ codes and distance accumulations depend on the lookup values). Even utilizing the state-of-the-art SIMD-optimized CPU implementation [1], the throughput peaks at roughly 1 GB/s per core when scanning PQ codes (1.2 GB/s on Intel(R) Xeon(R) Platinum 8259CL @ 2.50GHz). Within a core-memory-balanced server, the PQ code scanning process significantly underutilizes the available memory bandwidth, as about 16 cores are required to saturate the bandwidth of a single memory channel (around 20 GB/s).

On the other hand, GPUs present two primary limitations for large-scale vector search. Firstly, the limited memory capacity of individual GPUs makes large-scale searches on GPU clusters cost-prohibitive. For instance, accommodating only 1 TB of PQ codes would necessitate at least 16 NVIDIA A100 GPUs, each with 80 GB of memory, given that a portion of memory should be reserved for intermediate states during the search. These GPUs cost 300K USD in total¹ excluding the host servers. Although an alternative solution is to adopt a hybrid CPU-GPU architecture where the GPU fetches vectors from CPU's memory, the inter-processor bandwidth is way lower than the GPU memory bandwidth. Even for NVIDIA Grace Hopper, with the latest high-performance CPU-GPU interconnect, the single-direction bandwidth of 450 GB/s is only 15% of the GPU's bandwidth. Secondly, the throughput for PQ code scanning on GPUs is considerably lower than the GPU's bandwidth, only around 50% of the bandwidth even with large batch sizes (evaluated on NVIDIA V100), due to the multiple passes of memory accesses to write and read intermediate results at each search step [51].

¹Price on amazon.com as of October 2023.

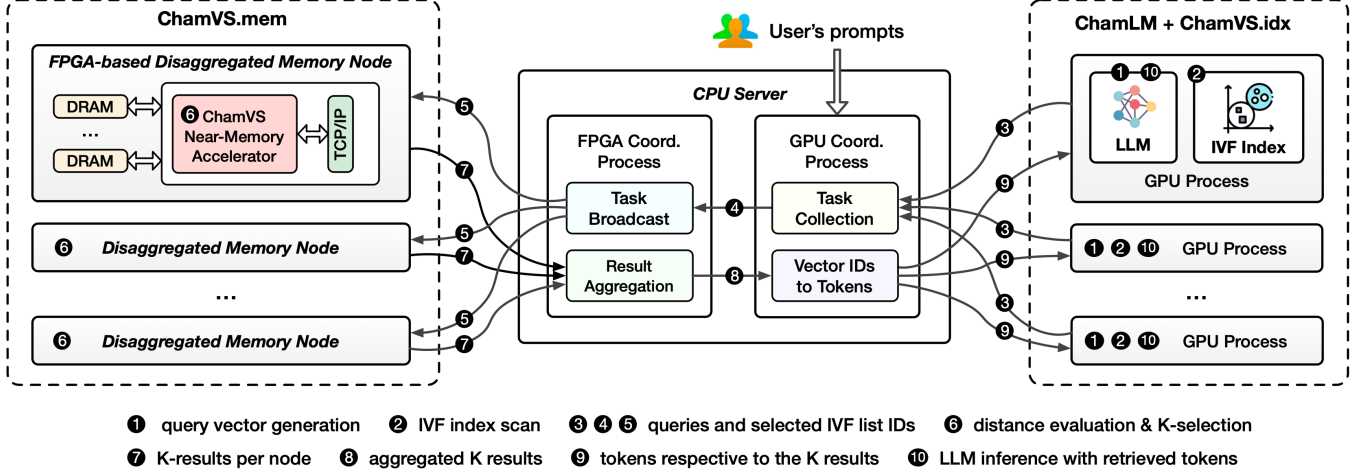


Figure 3: Chameleon integrates heterogeneous accelerators in a disaggregated architecture for high-performance and efficient RALM inference.

3 Chameleon: System Overview

We present Chameleon, a heterogeneous and disaggregated accelerator system for efficient, flexible, and high-performance RALM inference. **Chameleon addresses the system challenges in RALMs in the following ways:**

- Chameleon employs heterogeneous hardware to accelerate both LLM inference and vector search efficiently.
- Chameleon disaggregates the accelerators, enabling independent scaling for each type of hardware, thus supporting various RALM configurations efficiently.
- Though prototyped on FPGAs and GPUs, Chameleon’s modular design allows flexible hardware upgrades in the future, such as integrating more powerful LLM inference accelerators or ASIC-based ChamVS retrieval accelerators.

Figure 3 overviews the Chameleon architecture, which primarily consists of the following components.

Firstly, ChamLM is a multi-GPU LLM inference engine, as shown on the right side of Figure 3. Each GPU is managed by an independent GPU process. These processes can reside on either the same or different servers. Due to the significant reduction in LLM sizes by introducing a retriever [8, 68], ChamLM assigns each GPU a copy of the entire LLM, while larger models in the future can be implemented by simply extending ChamLM to support model parallelism across GPUs.

Secondly, ChamVS is a distributed and accelerated vector search engine. On the one hand, ChamVS.idx is a GPU-based IVF index scanner colocated with the ChamLM GPUs (right side of Figure 3). While the index scan can be executed on CPUs or FPGAs, GPUs are generally more favorable for handling such an embarrassingly parallel workload due to their

superior memory bandwidth and computational capability. Given that GPUs are already integrated into Chameleon, no additional devices are required. The only overhead is a minimal increase in GPU memory usage, because the index sizes, typically under one GB, are small enough compared to the vast memory footprints of the database vectors. On the other hand, ChamVS.mem is responsible for querying quantized database vectors. ChamVS.mem contains one or multiple disaggregated memory nodes, each with a partition of the database vectors and a near-memory retrieval accelerator prototyped on FPGA for query processing (left side of Figure 3).

Thirdly, a CPU server manages communication between the GPUs and FPGAs. It handles incoming search requests from the GPU processes, dispatches them to the FPGA-based disaggregated memory nodes, aggregates the per-partition results returned by the FPGAs, converts the K nearest neighbor vector IDs into their corresponding texts, and sends the retrieved tokens back to the GPUs.

Token generation workflow. For each token generation step, the procedure diverges depending on whether the retrieval is invoked. Without retrieval, the GPUs infer the next token as in regular LLMs. With retrieval, the first step is to generate a contextual query vector 1, either by using the hidden state of the current context [56, 57] or encoding the query tokens through another model [8]. Following this, the IVF index residing on the same GPU is scanned to select the $nprobe$ most relevant IVF lists 2. The query vector and the list IDs are then transmitted to the GPU coordinator process running on the CPU node via the network 3. After recording the association between queries and GPU IDs, the query and list IDs are forwarded to the FPGA coordination process 4, which broadcasts them to the FPGA-based disaggregated memory nodes 5. The ChamVS near-memory processor on each node then uses the query vectors to construct distance

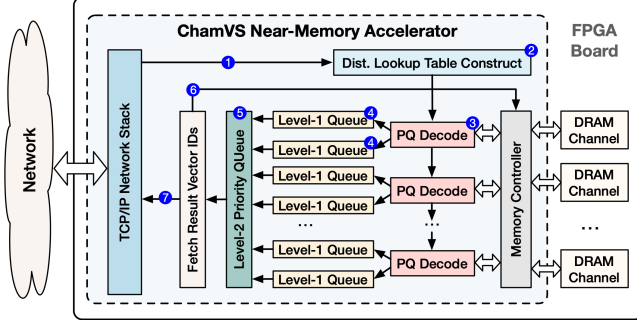


Figure 4: Each disaggregated memory node in ChamVS.mem contains a near-memory accelerator for efficient vector search.

lookup tables for each IVF list, computes the distances between the query and quantized database vectors, and collects the K nearest neighbors ⑥. Subsequently, the result vector IDs and distances from all memory nodes are sent back to the CPU server ⑦, which aggregates the results ⑧ and returns the tokens of the nearest neighbors to the originating GPU ⑨. Finally, the GPU predicts the next token based on both the context and the retrieved tokens ⑩.

4 Near-Memory Accelerator for Vector Search

ChamVS enables high-performance, large-scale vector search by pairing each disaggregated memory node with a near-memory accelerator. The FPGA prototype of a disaggregated memory node is shown in Figure 4, encompassing an on-chip hardware TCP/IP network stack, a distance lookup table construction unit, several PQ decoding units for evaluating distances between query vectors and quantized database vectors, a group of systolic priority queues for parallel K -selection, and multiple channels of DDR memory. In this section, we mainly elaborate on the PQ decoding units and the K -selection circuit, omitting the distance lookup table construction unit since it simply calculates L2 distances as introduced in § 2.

4.1 PQ Decoding Units

A PQ decoding unit reads quantized database vectors (PQ codes) from DRAM and computes the corresponding L2 distances to query vectors using a distance lookup table.

Figure 5 presents the design of a single PQ decoding unit, which can produce a result distance every clock cycle. We adopt a design with operator and pipeline parallelisms similar to [49, 64]. For each IVF list to scan, the unit first takes a distance lookup table as input and stores it in the BRAM (on-chip SRAM in FPGAs). The shape of the lookup table is $m \times 256$ for the typical 8-bit PQ codes ($2^8 = 256$), where m stands for the number of bytes per quantized vector. Different table columns are stored in separate BRAM slices, facilitating parallel distance lookups. Subsequently, the database PQ

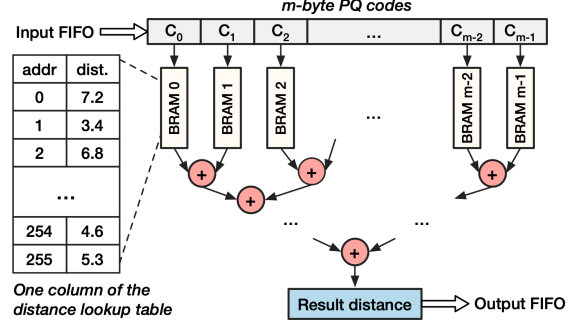


Figure 5: The design of a PQ decoding unit that evaluates distances between queries and quantized database vectors.

codes are loaded from DRAM and streamed to the PQ decoding unit via an m -byte-wide FIFO, with each byte serving as an address to retrieve a value from the corresponding column of the table. Upon completion of the m parallel table lookup operations, an adder tree sums up the values to produce the approximate distance between the query vector and the quantized database vector. The lookup and addition processes are pipelined such that the unit can consistently process m bytes of PQ codes and yield a result each clock cycle.

Multiple PQ decoding units operate in parallel to fully utilize the memory bandwidth, as shown in Figure 4 ③. The total number of units is determined by the quantization level m , the number of memory channels, and the width of the memory controller interface. For instance, given $m = 32$ and an FPGA comprising four memory channels, each accessible by a 64-byte-wide AXI interface to the memory controller, there would be $64 * 4 / 32 = 8$ PQ decoding units on the accelerator. When scanning a cluster of vectors, all units share the same distance lookup table, as each cluster is equally distributed across all memory channels. The units are arranged in a one-dimensional array, enabling each unit to forward the table to the subsequent one. This arrangement avoids a broadcasting topology, thus mitigating potential wire routing issues.

Summary: Thanks to the parallelism across and within PQ decoding units, query vectors can be rapidly compared against quantized database vectors in ChamVS.

4.2 Efficient K -Selection Module

Designing an efficient K -selection microarchitecture within ChamVS.mem presents significant challenges, as each PQ decoding unit generates one distance every clock cycle, requiring the K -selection module to manage multiple incoming elements per cycle. In this section, we begin by examining the register-array-based systolic priority queue, a building block for the K -selection module. However, instantiating many systolic priority queues of length K to satisfy throughput requirements proves too costly due to prohibitively high hardware

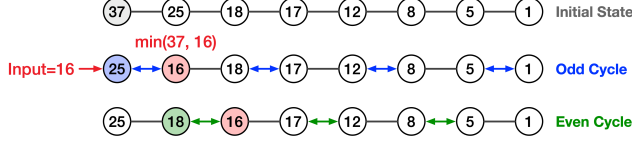


Figure 6: A systolic priority queue takes one input every two cycles.

resource consumption. Consequently, we propose the approximate hierarchical priority queue, a high-throughput, resource-efficient design for parallel K -selection on hardware.

4.2.1 Primitive: Systolic Priority Queue

Figure 6 shows the systolic priority queue [40, 65] for high-throughput replace operations (if the incoming element is smaller than the largest one in the queue, dequeue the latter and enqueue the incoming element). The systolic priority queue consists of a register array interconnected by compare-swap units, repeating a two-cycle procedure per replacement operation. During an odd cycle, the leftmost node is replaced with the minimum value between the existing leftmost value and an incoming element, followed by the swapping of all even entries in the array with their corresponding odd neighbors. In the subsequent even cycle, the swapping is reversed, with all the odd entries interchanging with the even ones. Throughout this process, the smallest element is gradually swapped to the rightmost position in the queue. The hardware resource consumption of such a priority queue scales linearly with its length, as both the number of registers and compare-swap units are proportional to the queue size.

A natural approach to implement K -selection in ChamVS is to instantiate a group of systolic priority queues in a hierarchical structure, as illustrated in Figure 4 4 5. Since a systolic priority queue can only ingest one input element every two cycles, yet the module should be capable of consuming all the distances produced by the PQ decoding units per cycle, two queues, termed as level-one (L1) queues, must be paired with one PQ decoding unit. Once all the database vectors have been scanned within a query, each L1 queue collects K elements. Subsequently, the level-two (L2) queue selects the final K results from L1 queues.

Unfortunately, a straightforward implementation of the hierarchical priority queue can consume an excessive amount of hardware resources, making the solution unaffordable even on high-end FPGAs. For example, a 100-element priority queue would utilize around 2.5% of lookup tables (LUTs) on the Alveo U250, one of AMD’s largest FPGA models. Given 32 instantiated PQ decoding units, the accelerator would necessitate 64 L1 queues to match the throughput of the decoding units, an amount that already exceeds the total LUT resources available on the FPGA. Consequently, it becomes imperative to devise a more resource-efficient approach for K -selection.

4.2.2 Approximate Hierarchical Priority Queue

We propose the approximate hierarchical priority queue architecture for high-performance and resource-efficient K -selection. Recognizing that the approximate nearest neighbor search inherently does not yield exact results, we relax the K -selection objective from selecting the K smallest distances in all queries to collecting precise results in the vast majority of cases, such as in 99% of the queries.

The intuition behind the approximate K -selection design is simple: it is unlikely that all the K results are produced by a single PQ decoding unit. For example, given 16 level-one queues with $K = 100$, the average number of the top 100 results in a queue is $100/16 = 6.25$. More specifically, the probability that one queue holds k of the K nearest neighbors can be formulated as $p(k) = C_K^k * (\frac{1}{\text{num_queue}})^k * (1 - \frac{1}{\text{num_queue}})^{K-k}$, where C_K^k represents the number of combinations selecting k out of K items. The cumulative probability that a queue contains no more than k of the K results can be calculated by $P(k) = \sum_{i=0}^k p(i)$. The probability distribution of p and P are visualized by the red bars and the blue curve in Figure 7, respectively. The figure demonstrates that it is highly unlikely that a queue holds more than 20 out of the $K=100$ results; thus, the length of the L1 priority queue can be truncated to 20 while producing almost the same results.

In our design, we aim to reduce the size of the L1 queues while ensuring that the results for 99% of queries remain identical to those obtained with an exact K -selection module. Specifically, for 99% of the queries, none of the L1 queues will omit any result that is supposed to be returned to the user.

Figure 8 shows the resource savings achieved by applying the approximate hierarchical priority queue. As the number of L1 queues increases, the queue sizes can be reduced by an order of magnitude while still retaining 99% of identical results. As the resource consumption of a queue is almost proportional to its length, such a reduction in size leads to a corresponding decrease in hardware resource consumption.

Summary: By minimizing the size of each queue, the approximate hierarchical priority queue architecture can match the high throughput of PQ decoding units while significantly reducing hardware resource consumptions.

4.3 Memory Management

ChamVS.mem manages several data components, including PQ codes, corresponding vector IDs, and metadata. Specifically, the PQ codes and vector IDs are stored in DRAM, while the metadata is loaded into BRAM during the system initialization phase. Since the entire memory space of a memory node is dedicated to vector search, ChamVS.mem operates directly in the physical address space, avoiding memory vir-

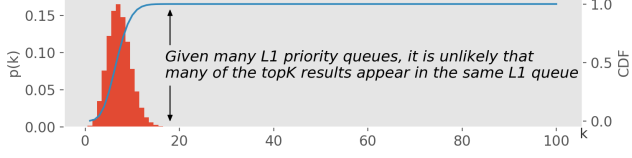


Figure 7: The probability distribution that one out of the 16 level-one priority queues holds k out of the top 100 nearest neighbors.

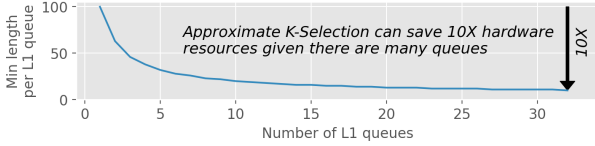


Figure 8: The proposed approximate hierarchical priority queue can save hardware resources by an order of magnitude.

tualization overheads. Because each vector cluster in the IVF index is typically big enough in large datasets, ChamVS.mem evenly distributes the quantized vectors and vector IDs within each cluster among all memory channels, such that the workloads per memory channel are well-balanced. Each memory channel has an AXI interface that bridges the memory controller and the compute logic, facilitating 64-byte data transmission per clock cycle. An address lookup table, as part of the metadata, records the starting physical address of PQ codes and vector IDs of each cluster. Additionally, the centroid vectors of the product quantizer constitute the other part of the metadata.

For distributed vector search, there are two approaches for data partitioning. The first way, which we apply in this paper, is to assign a portion of vectors in every IVF list to each memory node. For example, if there are four memory nodes and a thousand IVF lists, each memory node will hold all one thousand lists but only one-fourth of the vectors per list. In this case, the workload between memory nodes is always balanced: the coordinator sends the same scan request (list IDs) to all memory nodes, and the memory nodes scan the same amount of database vectors. This is practical in large-scale vector search, because each IVF list for a large dataset contains many vectors, and dividing a list into multiple shards will not turn sequential scans into random memory accesses. The second way is to assign a subset of IVF lists to a memory node such that different nodes hold distinct lists. This is suitable when each IVF list contains few vectors while there are many memory nodes. The scan workloads in this case are asymmetric between memory nodes, as it is possible that all the lists to scan happen to be on the same memory node.

Summary: ChamVS’s memory management mechanism (a) ensures a balanced load distribution across memory nodes and across memory channels within each node and (b) avoids memory virtualization overheads.

5 Implementation

Chameleon is implemented in 11K lines of code in total, including 3K lines of Vitis HLS C/C++ for the near-memory accelerator, 1.4K lines of C++ for the CPU coordination programs between GPUs and FPGAs, 3.5K lines of Python for the LM inference engine with the retrieval interface, and 3.2K lines of Python for various experiments and tests.

ChamLM. Referring to existing RALM research projects [56, 57], we build ChamLM on top of Fairseq [79], a language model toolkit based on PyTorch [80] that allows flexible instantiation of different LLM architectures and parameters. ChamLM extends Fairseq to support functionalities such as multi-GPU inference, initiating retrieval requests, integrating the retrieved tokens into the models, and TCP/IP network communication between the vector search engines and different GPU processes.

ChamVS. For ChamVS.idx, we use Faiss [51] to support such efficient index scan on both CPUs and GPUs. For ChamVS.mem, we develop the near-memory accelerator using Vitis HLS 2021.2 in C/C++ and integrate an open-source FPGA TCP/IP network stack [36] that connects to the accelerator kernel. The coordinator process between ChamVS.idx and ChamVS.mem for query broadcasting and result aggregation is implemented using C/C++ and the socket library.

6 Evaluation

We evaluate Chameleon to answer the following questions:

1. How much performance benefit can ChamVS attain in large-scale vector search? (§ 6.2)
2. What are the energy and hardware resource consumptions of the ChamVS near-memory accelerator? (§ 6.2)
3. How does Chameleon perform across different RALMs by introducing heterogeneous accelerators? (§ 6.3)
4. Is accelerator disaggregation necessary? (§ 6.3)

6.1 Experimental Setup

LLMs. We evaluate RALM models of similar sizes to those in existing RALM research [8, 42, 72, 89, 104], from 100 million to more than one billion parameters. For each decoder-only (Dec) and encoder-decoder (EncDec) RALM, we experiment

Table 2: Decoder-only and encoder-decoder RALMs for evaluation.

	Dim.	Layers	Heads	Param.	Interval	K
Dec-S	512	24	8	101M	1	100
Dec-L	1024	96	16	1259M	1	100
EncDec-S	512	2,24	8	158M	8/64/512	10
EncDec-L	1024	2,96	16	1738M	8/64/512	10

Table 3: The vector datasets used in the evaluation.

	Deep	SIFT	SYN-512	SYN-1024
#vec	1E+9	1E+9	1E+9	1E+9
D	96	128	512	1,024
m	16	16	32	64
$nlist$	32,768	32,768	32,768	32,768
Raw vectors (GB)	384	512	2,048	4,096
PQ and vec ID (GB)	24	24	40	72

with a smaller model (S) and a larger model (L). Table 2 summarizes the four RALMs for evaluation, including input dimensionalities, numbers of layers and attention heads, model sizes, retrieval intervals, and neighbor numbers. For encoder-decoder models, we follow [8] to use a two-layer shallow encoder and a deeper decoder, and set different retrieval intervals. For all the models, we use a vocabulary size of 50K and let them generate 512 tokens per sequence.

Vector datasets. For large-scale vector search, we use two real-world datasets and two synthetic datasets as summarized in Table 3. Specifically, the SIFT and Deep datasets are the most popular benchmarks for billion-scale ANN, each with 10K query vectors. Due to the lack of openly available vector datasets for RALM, we create two synthetic datasets by replicating each SIFT vector to the models’ dimensionalities (512 and 1024), such that they can also be used in RALM inference experiments. As a common practice, we set $nlist$, the number of clusters in the IVF index, to approximately the square root of the number of vectors in the dataset ($nlist=32K$). We set $nprobe$ as 32 to scan 0.1% of database vectors per query, for which high recall can be achieved on both real-world datasets ($R@100=93\%$ on Deep and $R@100=94\%$ on SIFT). We quantize the SIFT and Deep datasets to 16-byte PQ codes, while the two synthetic datasets adopt 32 and 64-byte PQ codes, respectively, due to their higher dimensionalities.

Software. For vector search, we use *Faiss* [1] (v1.7.2) developed by Meta as the baseline software. *Faiss* is currently the most popular PQ-based ANN library, known for its highly optimized implementations for both CPUs and GPUs. For LLM inference, we extend Fairseq [79] as introduced in § 5.

Hardware. We instantiate the ChamVS near-memory accelerator on AMD Alveo U250 FPGAs (16 nm) equipped with 64 GB of DDR4 memory (4 channels x 16 GB) and set

the accelerator frequency to 140 MHz. For a fair comparison, each ChamVS memory node is compared to a CPU-based vector search system with equivalent memory capacity (64 GB) and an 8-core AMD EPYC 7313 processor (7 nm) with a base frequency of 3.0 GHz and a max turbo frequency of 3.7 GHz. We evaluate NVIDIA RTX 3090 GPUs (8nm) with 24 GB GDDR6X memory. As we will show later, ChamVS can achieve better performance and energy efficiency even if instantiated on FPGAs manufactured in an older technology.

6.2 Vector Search on ChamVS

Performance. We compare ChamVS with baseline systems on four large-scale vector datasets, each using four different configurations: searching solely on CPU (CPU), scanning the IVF index on GPU and the PQ codes on CPU (CPU-GPU), scanning the index on CPU and the PQ codes on FPGA (FPGA-CPU), and scanning the index on GPU and the PQ codes on FPGA (FPGA-GPU). To report the best baseline performance, the CPU and CPU-GPU systems are monolithic, while the FPGA-CPU and FPGA-GPU systems are disaggregated over the network. Figure 9 shows the vector search latency distributions of different batch sizes using the four solutions. Each white dot in the violin plots denotes a median latency. The number of CPU cores and the number of accelerators used are listed in the plot legends. We make two primary observations from the experiments:

Firstly, the near-memory accelerator in ChamVS results in significantly lower vector search latency compared to the CPU baseline. Across different datasets and batch sizes (Figure 9), the FPGA-CPU solution achieves $1.36\sim 6.13\times$ speedup compared to the CPU baseline, and the FPGA-GPU solution shows even higher speedup ($2.25\sim 23.72\times$). This is because the ChamVS near memory accelerator can (a) decode PQ codes in parallel, (b) pipeline the decoding, distance calculation, and K-selection, such that each quantized vector can be processed by the pipeline with an initiation interval of a single clock cycle. Such specialization leads to significantly better performance compared to CPUs in scanning PQ code and selecting the K nearest neighbors.

Secondly, scanning the IVF index on GPU allows further latency improvements compared to the FPGA-CPU solution. The FPGA-GPU solution does not require additional GPUs as they are inherently available in RALM systems. As shown in Figure 9, the FPGA-GPU approach achieves $1.04\sim 3.87\times$ speedup compared to the FPGA-CPU solution. This is because the IVF index scan procedure can easily leverage the massively parallelism and the high memory bandwidth of GPUs: the query vectors are compared against all index centroid vectors, and the $nprobe$ closest centroids are selected. In contrast, the hybrid CPU-GPU solution shows little or even negative improvements compared to the CPU-only solution ($0.91\sim 1.42\times$), because the search performance is limited by the slow PQ code scan process on CPU.

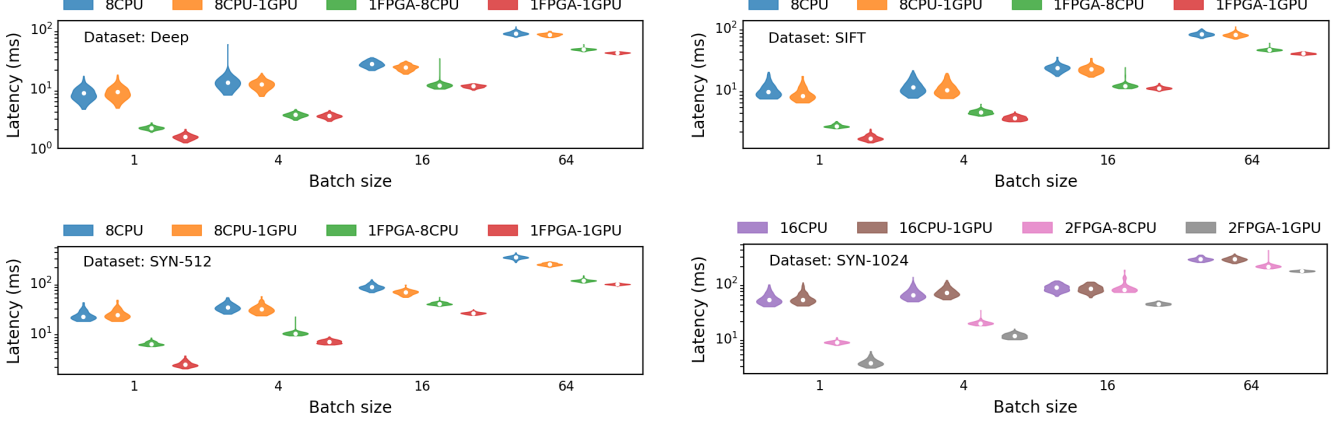


Figure 9: ChamVS achieves significantly lower vector search latency than CPUs and GPUs.

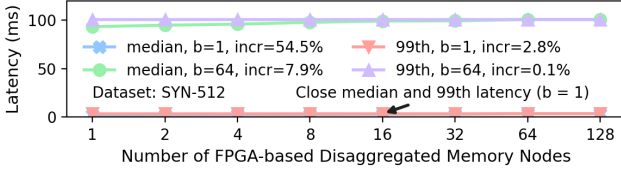


Figure 10: The query latencies when scaling out memory nodes.

Scalability. We extrapolate query latency beyond the limited number of accelerators available in our evaluation. Considering the one-GPU and N -FPGA setup, we estimate the latency distribution by summing up accelerator and network latencies. Given a query on N FPGAs, an accelerator latency sample is the maximum of N randomly sampled latency numbers from the 1-FPGA setup. For network latency, we assume a 100 Gbps bandwidth for the CPU server and apply the LogGP model [2, 21], which assumes a tree topology for broadcast and reduce communications, setting the latency between two endpoints as $10.0 \mu\text{s}$ (a conservative number compared to $6.0 \mu\text{s}$ reported in [37, 38]). Figure 10 presents the median and the 99th percentile latencies for different batches on the SYN-512 dataset. The tail latencies remain almost identical to those in the one-node setup due to the negligible network latency compared to the query. As for the median latencies, there is only a 7.9% increase for a batch size of 64, while for the case without batching, the latency increases by 54.5% as the accelerator latency is determined by the slowest one.

Resource and energy consumption. For the FPGA-based near-memory accelerator, we report the resource and energy consumption using Vivado. For CPUs and GPUs, we measure their energy consumption using *Intel RAPL* and *NVIDIA System Management Interface*, respectively.

The ChamVS near-memory accelerator consumes few

Table 4: The retrieval accelerator consumes little FPGA resources.

Dataset	LUT	FF	BRAM	URAM	DSP
SIFT	25.3%	16.2%	13.7%	4.4%	12.2%
Deep	23.7%	15.4%	13.0%	4.4%	10.4%
SYN-512	23.2%	15.5%	23.2%	4.4%	8.4%
SYN-1024	28.0%	19.0%	35.7%	4.4%	11.9%

Table 5: Average energy consumption per query (in mJ) on ChamVS and CPUs using various batch sizes (1~16).

	CPU			ChamVS (FPGA + GPU)		
	b=1	b=4	b=16	b=1	b=4	b=16
SIFT	950.3	434.0	143.3	53.6	28.2	21.5
Deep	929.5	412.9	141.9	52.3	26.9	20.5
SYN-512	1734.9	957.8	372.5	95.6	55.0	41.1
SYN-1024	4459.9	2315.0	918.5	170.1	107.8	85.2

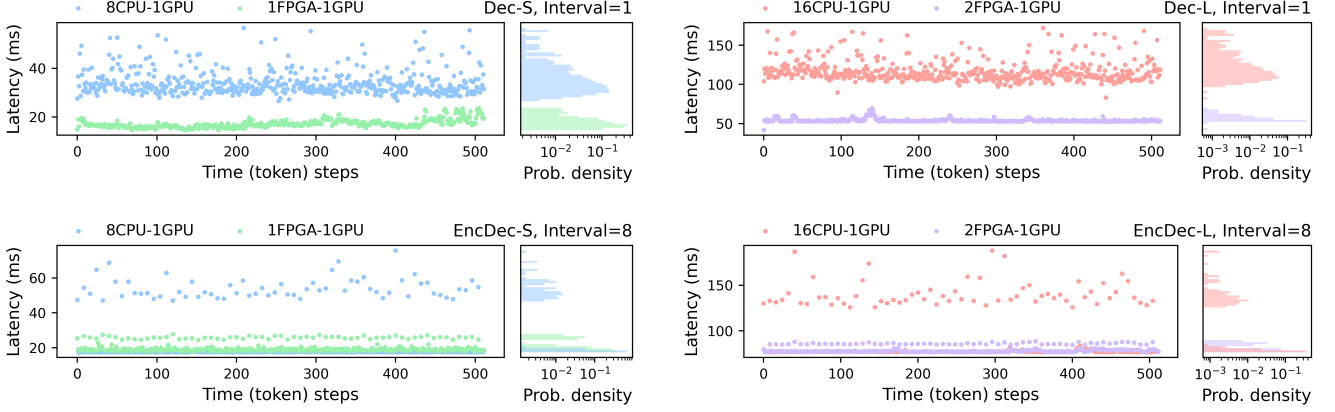


Figure 11: RALM inference latency given different LLM configurations and retrieval intervals.

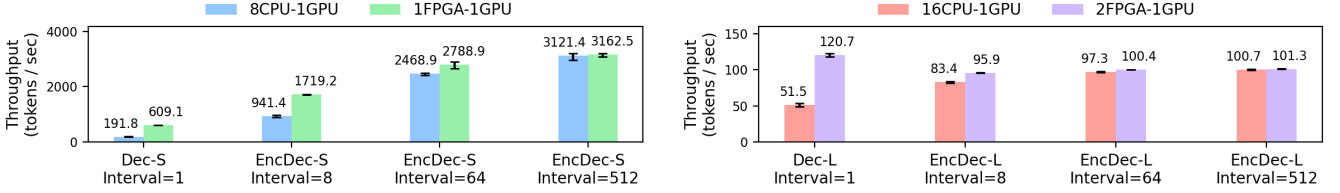


Figure 12: RALM inference throughput given different LLM configurations and retrieval intervals.

FPGA resources. The AMD Alveo U250 FPGA contains 1.4M Lookup-Tables (LUTs), 2.9M Flip-Flops (FFs), 2.1K Block-RAM (BRAM), 1.3K Ultra-RAM (URAM), and 12K Digital Signal Processors (DSPs), and four memory channels. As shown in Table 4, the accelerator only consumes around 20% of the hardware resources.

Considering its low hardware resource consumption, there are two approaches to further improve the cost-efficiency of ChamVS. Firstly, one can implement the accelerator on an FPGA device with a higher ratio of memory channels to FPGA resources. For example, using an FPGA chip identical to the U250 device, increasing the number of memory channels to, e.g., 12, would lead to around $3\times$ PQ-code scan performance. This is feasible because high-end FPGAs have enough I/O pins even for HBM that has much higher bandwidth [99]. Secondly, it would be beneficial to increase the memory capacity per FPGA. Instead of using the U250 FPGA with only 64 GB DRAM, one can increase the memory capacity per FPGA board so that fewer FPGAs are needed in Chameleon to serve a large dataset. For example, Enzian [20] is an academic FPGA platform equipped with up to 1 TB of DRAM per device.

ChamVS achieves $5.8\sim 26.2\times$ energy efficiency compared to the CPU. Table 5 summarizes the average energy consumption (in mJ) of different systems to serve a single query across different batch sizes. For ChamVS, we report the energy per query by measuring the power consumption times latency for

scanning index on GPU and scanning PQ codes on FPGAs, respectively, and summing the two parts up.

6.3 End-to-end RALM Inference on Chameleon

In this section, we evaluate the end-to-end RALM inference performance on Chameleon with different model configurations and retrieval intervals. We use the SYN-512 and SYN-1024 datasets for the smaller and larger models, respectively.

Performance. For both latency and throughput evaluation, we evaluate system performance when generating a 512-token sequence using a single GPU for LLM inference, and each experiment is conducted three times. For the latency evaluation, we disable batching, while for the throughput evaluation, we set the batch size as the maximum allowed given the GPU’s memory capacity (batch size = 64 for Dec-S and EncDec-S; 8 for Dec-L and EncDec-L) and assume that all sequences in the batch will finish generating 512 consecutive tokens, given that early termination for a subset of sequences can be easily addressed via preemptive scheduling [62]. For vector search in RALM, we use the FPGA-GPU solution for ChamVS and the CPU-only solution as the baseline, since the CPU-GPU vector search engine can be even slower using small batches.

Chameleon significantly outperforms the CPU-GPU baseline system in latency for inference steps involving vector search. Figure 11 compares the RALM inference latency

between Chameleon (FPGA-GPU) and the baseline system (CPU-GPU). The left column shows the small models (Dec-S and EncDec-S), while the right column shows the large models. Each row uses the same retrieval interval (one and eight). For each plot, the left subplot shows the latency over token generation steps, while the right one depicts the latency distribution. While the LLM inference is still executed on the GPU, the FPGA-GPU retrieval engine significantly reduces the latency at the token generation steps requiring retrieval. Specifically, the speedup provided by Chameleon at retrieval-based inference steps (retrieval + inference) ranges from $1.94\sim 4.11\times$, $1.71\sim 3.02\times$, $1.76\sim 3.41\times$, and $1.29\sim 2.13\times$ for Dec-S, EncDec-S, Dec-L, and EncDec-L, respectively.

Chameleon achieves up to $3.18\times$ throughput compared to the CPU-GPU baseline system. As shown in Figure 12, the lower the retrieval interval, the higher throughput advantage Chameleon can offer, with the speedup being $3.18\times$ and $2.34\times$ for Dec-S and Dec-L that require retrieval per token generation (interval = 1). Chameleon attains greater speedup in batched inference than single-sequence inference as in the latency experiments. This is because, as the batch size grows, the latency increase for LLM inference is not as significant as that of vector search, due to the many-core parallelism offered by the GPU during LLM inference. Thus, the speedup observed in batched inference is closer to that of vector search than in single-sequence inference.

The need for resource disaggregation. Given the broad range of configurations in RALMs — such as different model sizes, retrieval intervals, and database sizes — it is likely that either the LLM inference or vector search engine will be underutilized if the hardware resource ratio is not carefully configured. Based on the evaluated batched inference throughput, Figure 13 shows that the number of GPUs required to saturate the ChamVS vector search engine can vary dramatically, ranging from 0.2 to 442. This makes a monolithic design approach, which entails installing a fixed number of accelerators on a single server, both inflexible and sometimes impractical (a single server cannot accommodate 442 accelerators). Chameleon’s disaggregated architecture addresses this issue by allowing for flexible combinations of hardware resources over the network, thereby enhancing overall accelerator utilization.

In future cloud deployments of such a disaggregated accelerator system, resource sharing across users is also an option to enhance resource utilization. For example, ChamVS can be wrapped as a service accessible by multiple users, each operating an RALM on one or more GPUs. This approach allows the vector search accelerators to be better utilized even for models of low retrieval frequencies.

7 Related Work

To the best of our knowledge, Chameleon represents the first endeavor to analyze retrieval-augmented language models

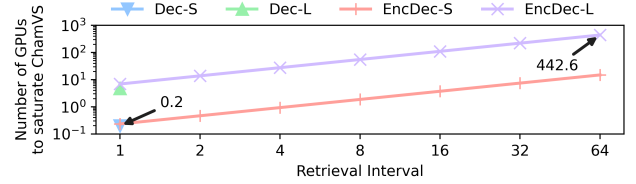


Figure 13: The optimal accelerator ratio to saturate both types of accelerators given different RALM configurations.

from a systems perspective, addressing associated challenges via a heterogeneous and disaggregated accelerator architecture. We proceed to introduce research on related topics below.

Resource disaggregation. Resource disaggregation has become increasingly popular in data centers. CPUs, memory, storage, and accelerators are connected through a high-speed network [24], such that these resources can be combined according to system needs without overprovisioning any type of the resources [26, 55, 73, 74]. The flexible introduction of extra resources, such as remote memory, helps in system performance compared to servers with monolithic designs [5, 107].

Near data processing. Data movements from memory or storage devices to processors are expensive, thus various literature has proposed to offload some computation workloads to a processor near or within memory/storage [23, 59, 78, 88, 90, 94, 96]. This approach is especially effective for data-intensive applications because the offloaded compute logic is simple, and a large portion of data is filtered out near memory/storage before being sent to CPUs. Typical use cases include database systems [23, 50], big data processing [32, 52, 53], recommender systems [47, 48, 102], time series processing [25], and genome sequence analysis [75]. The processors near the data can be regular CPUs [3], vector processors [81], reconfigurable hardware [29, 60], or ASICs [75].

AI accelerators. GPUs are commonly used for deep learning acceleration nowadays [18, 41, 98]. Alternative specialized architectures have also been implemented on FPGAs [6, 27, 77, 82, 92, 109] and ASICs [30, 34, 54, 61, 91, 108]. These accelerators are often co-designed with algorithm relaxations such as neural network pruning and quantization [28, 35, 69, 70]. Compiler-based solutions are also necessary to reduce the programming effort to map tensor programs to the various hardware backends [14, 63].

Vector search on modern hardware. Google proposes to accelerate exact nearest neighbor search on TPUs and show great performance on small datasets [17]. Similarly, the exact search can be implemented on FPGAs [105]. For ANN search, the most popular GPU-accelerated library so far is Faiss developed by Meta [51], and there are several academic GPU implementations [15, 16, 101]. Lee et al. [64] study ASIC designs for IVF-PQ, and the simulation-based eval-

uation shows significant speedup over GPUs. A couple of works [49, 106] implement IVF-PQ on an FPGA, but their designs are constrained by either the limited HBM capacity or the slow CPU-FPGA interconnect. In contrast, Chameleon disaggregates IVF-PQ, with the index on GPUs and PQ codes on FPGA-based memory nodes, and employs the innovative hardware priority queue design to achieve high performance with little hardware resources, even for large neighbor numbers. Apart from accelerator-based solutions, researchers also study modern storage for vector search. Hu et al. [39] propose to push down vector distance evaluation to NAND flash to reduce data movement. Ren et al. [87] suggest storing vectors in non-volatile memory to scale up graph-based ANN, while on-disk ANN has to be careful with I/O cost [13, 45, 66]. The emerging CXL technology has introduced another level of memory hierarchy as an option for ANN search [44].

8 Conclusion

Retrieval-augmented language models offer compelling advantages but also present unique system design challenges. To address these problems, we introduce Chameleon, an efficient RALM inference engine that leverages (a) accelerator heterogeneity for high-performance language model inference and vector retrieval and (b) accelerator disaggregation for system flexibility and resource efficiency. Our Chameleon prototype, implemented on a heterogeneous cluster of CPUs, GPUs, and FPGAs achieves up to $3.18\times$ speedup in throughput compared to existing state-of-the-art systems. These promising results validate the effectiveness of the proposed design principles, specifically the integration of accelerator heterogeneity and disaggregation, paving the way for the adoption of these principles in future-generation RALM systems.

References

- [1] Faiss. <https://github.com/facebookresearch/faiss/>.
- [2] Albert Alexandrov, Mihai F Ionescu, Klaus E Schauser, and Chris Scheiman. Loggp: Incorporating long messages into the logp model—one step closer towards a realistic model for parallel computation. In *Proceedings of the seventh annual ACM symposium on Parallel algorithms and architectures*, pages 95–105, 1995.
- [3] Mohammad Alian, Seung Won Min, Hadi Asghari-moghaddam, Ashutosh Dhar, Dong Kai Wang, Thomas Roewer, Adam McPadden, Oliver O’Halloran, Deming Chen, Jinjun Xiong, et al. Application-transparent near-memory processing architecture with memory channel network. In *2018 51st Annual IEEE/ACM International Symposium on Microarchitecture (MICRO)*, pages 802–814. IEEE, 2018.
- [4] Uri Alon, Frank Xu, Junxian He, Sudipta Sengupta, Dan Roth, and Graham Neubig. Neuro-symbolic language modeling with automaton-augmented retrieval. In *International Conference on Machine Learning*, pages 468–485. PMLR, 2022.
- [5] Emmanuel Amaro, Christopher Branner-Augmon, Zhihong Luo, Amy Ousterhout, Marcos K Aguilera, Aurojit Panda, Sylvia Ratnasamy, and Scott Shenker. Can far memory improve job throughput? In *Proceedings of the Fifteenth European Conference on Computer Systems*, pages 1–16, 2020.
- [6] Aman Arora, Samidh Mehta, Vaughn Betz, and Lizy K John. Tensor slices to the rescue: Supercharging ml acceleration on fpgas. In *The 2021 ACM/SIGDA International Symposium on Field-Programmable Gate Arrays*, pages 23–33, 2021.
- [7] Emily M Bender, Timnit Gebru, Angelina McMillan-Major, and Shmargaret Shmitchell. On the dangers of stochastic parrots: Can language models be too big? In *Proceedings of the 2021 ACM conference on fairness, accountability, and transparency*, pages 610–623, 2021.
- [8] Sebastian Borgeaud, Arthur Mensch, Jordan Hoffmann, Trevor Cai, Eliza Rutherford, Katie Millican, George Bm Van Den Driessche, Jean-Baptiste Lespiau, Bogdan Damoc, Aidan Clark, et al. Improving language models by retrieving from trillions of tokens. In *International conference on machine learning*, pages 2206–2240. PMLR, 2022.
- [9] Lucas Bourtole, Varun Chandrasekaran, Christopher A Choquette-Choo, Hengrui Jia, Adelin Travers, Baiwu Zhang, David Lie, and Nicolas Papernot. Machine unlearning. In *2021 IEEE Symposium on Security and Privacy (SP)*, pages 141–159. IEEE, 2021.
- [10] Tom Brown, Benjamin Mann, Nick Ryder, Melanie Subbiah, Jared D Kaplan, Prafulla Dhariwal, Arvind Neelakantan, Pranav Shyam, Girish Sastry, Amanda Askell, et al. Language models are few-shot learners. *Advances in neural information processing systems*, 33:1877–1901, 2020.
- [11] Nicholas Carlini, Florian Tramèr, Eric Wallace, Matthew Jagielski, Ariel Herbert-Voss, Katherine Lee, Adam Roberts, Tom Brown, Dawn Song, Ulfar Erlingsson, et al. Extracting training data from large language models. In *30th USENIX Security Symposium (USENIX Security 21)*, pages 2633–2650, 2021.
- [12] Min Chen, Zhikun Zhang, Tianhao Wang, Michael Backes, Mathias Humbert, and Yang Zhang. When

- machine unlearning jeopardizes privacy. In *Proceedings of the 2021 ACM SIGSAC conference on computer and communications security*, pages 896–911, 2021.
- [13] Qi Chen, Bing Zhao, Haidong Wang, Mingqin Li, Chuanjie Liu, Zengzhong Li, Mao Yang, and Jingdong Wang. Spann: Highly-efficient billion-scale approximate nearest neighbor search. *arXiv preprint arXiv:2111.08566*, 2021.
- [14] Tianqi Chen, Thierry Moreau, Ziheng Jiang, Lianmin Zheng, Eddie Yan, Haichen Shen, Meghan Cowan, Leyuan Wang, Yuwei Hu, Luis Ceze, et al. {TVM}: An automated {End-to-End} optimizing compiler for deep learning. In *13th USENIX Symposium on Operating Systems Design and Implementation (OSDI 18)*, pages 578–594, 2018.
- [15] Wei Chen, Jincal Chen, Fuhao Zou, Yuan-Fang Li, Ping Lu, Qiang Wang, and Wei Zhao. Vector and line quantization for billion-scale similarity search on gpus. *Future Generation Computer Systems*, 99:295–307, 2019.
- [16] Wei Chen, Jincal Chen, Fuhao Zou, Yuan-Fang Li, Ping Lu, and Wei Zhao. Robustiq: A robust ann search method for billion-scale similarity search on gpus. In *Proceedings of the 2019 on International Conference on Multimedia Retrieval*, pages 132–140, 2019.
- [17] Felix Chern, Blake Hechtman, Andy Davis, Ruiqi Guo, David Majnemer, and Sanjiv Kumar. Tpu-knn: K nearest neighbor search at peak flop/s. *arXiv preprint arXiv:2206.14286*, 2022.
- [18] Seungbeom Choi, Sunho Lee, Yeonjae Kim, Jongse Park, Youngjin Kwon, and Jaehyuk Huh. Serving heterogeneous machine learning models on {Multi-GPU} servers with {Spatio-Temporal} sharing. In *2022 USENIX Annual Technical Conference (USENIX ATC 22)*, pages 199–216, 2022.
- [19] Aakanksha Chowdhery, Sharan Narang, Jacob Devlin, Maarten Bosma, Gaurav Mishra, Adam Roberts, Paul Barham, Hyung Won Chung, Charles Sutton, Sebastian Gehrmann, et al. Palm: Scaling language modeling with pathways. *arXiv preprint arXiv:2204.02311*, 2022.
- [20] David Cock, Abishek Ramdas, Daniel Schwyn, Michael Giardino, Adam Turowski, Zhenhao He, Nora Hossle, Dario Korolija, Melissa Licciardello, Kristina Martsenko, et al. Enzian: an open, general, cpu/fpga platform for systems software research. In *Proceedings of the 27th ACM International Conference on Architectural Support for Programming Languages and Operating Systems*, pages 434–451, 2022.
- [21] David Culler, Richard Karp, David Patterson, Abhijit Sahay, Klaus Erik Schauser, Eunice Santos, Ramesh Subramonian, and Thorsten Von Eicken. Logp: Towards a realistic model of parallel computation. In *Proceedings of the fourth ACM SIGPLAN symposium on Principles and practice of parallel programming*, pages 1–12, 1993.
- [22] Jacob Devlin, Ming-Wei Chang, Kenton Lee, and Kristina Toutanova. Bert: Pre-training of deep bidirectional transformers for language understanding. *arXiv preprint arXiv:1810.04805*, 2018.
- [23] Jaeyoung Do, Yang-Suk Kee, Jignesh M Patel, Chanik Park, Kwanghyun Park, and David J DeWitt. Query processing on smart ssds: Opportunities and challenges. In *Proceedings of the 2013 ACM SIGMOD International Conference on Management of Data*, pages 1221–1230, 2013.
- [24] Aleksandar Dragojević, Dushyanth Narayanan, Miguel Castro, and Orion Hodson. {FaRM}: Fast remote memory. In *11th USENIX Symposium on Networked Systems Design and Implementation (NSDI 14)*, pages 401–414, 2014.
- [25] Ivan Fernandez, Ricardo Quisilant, Eladio Gutiérrez, Oscar Plata, Christina Giannoula, Mohammed Alser, Juan Gómez-Luna, and Onur Mutlu. Natsa: a near-data processing accelerator for time series analysis. In *2020 IEEE 38th International Conference on Computer Design (ICCD)*, pages 120–129. IEEE, 2020.
- [26] Henrique Fingler, Zhiting Zhu, Esther Yoon, Zhipeng Jia, Emmett Witchel, and Christopher J Rossbach. Dgsf: Disaggregated gpus for serverless functions. In *2022 IEEE International Parallel and Distributed Processing Symposium (IPDPS)*, pages 739–750. IEEE, 2022.
- [27] Jeremy Fowers, Kalin Ovtcharov, Michael Papamichael, Todd Massengill, Ming Liu, Daniel Lo, Shlomi Alkalay, Michael Haselman, Logan Adams, Mahdi Ghandi, et al. A configurable cloud-scale dnn processor for real-time ai. In *2018 ACM/IEEE 45th Annual International Symposium on Computer Architecture (ISCA)*, pages 1–14. IEEE, 2018.
- [28] Elias Frantar, Saleh Ashkboos, Torsten Hoeftler, and Dan Alistarh. Gptq: Accurate post-training quantization for generative pre-trained transformers. *arXiv preprint arXiv:2210.17323*, 2022.
- [29] Mingyu Gao and Christos Kozyrakis. Hrl: Efficient and flexible reconfigurable logic for near-data processing. In *2016 IEEE International Symposium on High Performance Computer Architecture (HPCA)*, pages 126–137. Ieee, 2016.

- [30] Mingyu Gao, Jing Pu, Xuan Yang, Mark Horowitz, and Christos Kozyrakis. Tetris: Scalable and efficient neural network acceleration with 3d memory. In *Proceedings of the Twenty-Second International Conference on Architectural Support for Programming Languages and Operating Systems*, pages 751–764, 2017.
- [31] Tiezheng Ge, Kaiming He, Qifa Ke, and Jian Sun. Optimized product quantization. *IEEE transactions on pattern analysis and machine intelligence*, 36(4):744–755, 2013.
- [32] Boncheol Gu, Andre S Yoon, Duck-Ho Bae, Insoon Jo, Jinyoung Lee, Jonghyun Yoon, Jeong-Uk Kang, Moon-sang Kwon, Chanhoo Yoon, Sangyeun Cho, et al. Bis-cuit: A framework for near-data processing of big data workloads. *ACM SIGARCH Computer Architecture News*, 44(3):153–165, 2016.
- [33] Kelvin Guu, Kenton Lee, Zora Tung, Panupong Pasupat, and Mingwei Chang. Retrieval augmented language model pre-training. In *International conference on machine learning*, pages 3929–3938. PMLR, 2020.
- [34] Tae Jun Ham, Sung Jun Jung, Seonghak Kim, Young H Oh, Yeonhong Park, Yoonho Song, Jung-Hun Park, Sanghee Lee, Kyoung Park, Jae W Lee, et al. A³: Accelerating attention mechanisms in neural networks with approximation. In *2020 IEEE International Symposium on High Performance Computer Architecture (HPCA)*, pages 328–341. IEEE, 2020.
- [35] Song Han, Huizi Mao, and William J Dally. Deep compression: Compressing deep neural networks with pruning, trained quantization and Huffman coding. *arXiv preprint arXiv:1510.00149*, 2015.
- [36] Zhenhao He, Dario Korolija, and Gustavo Alonso. Easynet: 100 gbps network for hls. In *2021 31th International Conference on Field Programmable Logic and Applications (FPL)*, 2021.
- [37] Torsten Hoefler, Andre Lichei, and Wolfgang Rehm. Low-overhead loggp parameter assessment for modern interconnection networks. In *2007 IEEE International Parallel and Distributed Processing Symposium*, pages 1–8. IEEE, 2007.
- [38] Torsten Hoefler and Dmitry Moor. Energy, memory, and runtime tradeoffs for implementing collective communication operations. *Supercomputing frontiers and innovations*, 1(2):58–75, 2014.
- [39] Han-Wen Hu, Wei-Chen Wang, Yuan-Hao Chang, Yung-Chun Lee, Bo-Rong Lin, Huai-Mu Wang, Yen-Po Lin, Yu-Ming Huang, Chong-Ying Lee, Tzu-Hsiang Su, et al. Ice: An intelligent cognition engine with 3d NAND-based in-memory computing for vector similarity search acceleration. In *2022 55th IEEE/ACM International Symposium on Microarchitecture (MICRO)*, pages 763–783. IEEE, 2022.
- [40] Muhuan Huang, Kevin Lim, and Jason Cong. A scalable, high-performance customized priority queue. In *2014 24th International Conference on Field Programmable Logic and Applications (FPL)*, pages 1–4. IEEE, 2014.
- [41] Andrei Ivanov, Nikoli Dryden, Tal Ben-Nun, Shigang Li, and Torsten Hoefler. Data movement is all you need: A case study on optimizing transformers. *Proceedings of Machine Learning and Systems*, 3:711–732, 2021.
- [42] Gautier Izacard and Edouard Grave. Leveraging passage retrieval with generative models for open domain question answering. *arXiv preprint arXiv:2007.01282*, 2020.
- [43] Gautier Izacard, Patrick Lewis, Maria Lomeli, Lucas Hosseini, Fabio Petroni, Timo Schick, Jane Dwivedi-Yu, Armand Joulin, Sebastian Riedel, and Edouard Grave. Few-shot learning with retrieval augmented language models. *arXiv preprint arXiv:2208.03299*, 2022.
- [44] Junhyeok Jang, Hanjin Choi, Hanyeoreum Bae, Seungjun Lee, Miryeong Kwon, and Myoungsoo Jung. {CXL-ANNS}:{Software-Hardware} collaborative memory disaggregation and computation for {Billion-Scale} approximate nearest neighbor search. In *2023 USENIX Annual Technical Conference (USENIX ATC 23)*, pages 585–600, 2023.
- [45] Suhas Jayaram Subramanya, Fnu Devvrit, Harsha Vardhan Simhadri, Ravishankar Krishnawamy, and Rohan Kadekodi. Diskann: Fast accurate billion-point nearest neighbor search on a single node. *Advances in Neural Information Processing Systems*, 32, 2019.
- [46] Herve Jegou, Matthijs Douze, and Cordelia Schmid. Product quantization for nearest neighbor search. *IEEE transactions on pattern analysis and machine intelligence*, 33(1):117–128, 2010.
- [47] Wenqi Jiang, Zhenhao He, Shuai Zhang, Thomas B Preußer, Kai Zeng, Liang Feng, Jiansong Zhang, Tongxuan Liu, Yong Li, Jingren Zhou, et al. Microrec: efficient recommendation inference by hardware and data structure solutions. *Proceedings of Machine Learning and Systems*, 3:845–859, 2021.
- [48] Wenqi Jiang, Zhenhao He, Shuai Zhang, Kai Zeng, Liang Feng, Jiansong Zhang, Tongxuan Liu, Yong Li, Jingren Zhou, Ce Zhang, et al. Fleetrec: Large-scale

- recommendation inference on hybrid gpu-fpga clusters. In *Proceedings of the 27th ACM SIGKDD Conference on Knowledge Discovery & Data Mining*, pages 3097–3105, 2021.
- [49] Wenqi Jiang, Shigang Li, Yu Zhu, Johannes de Fine Licht, Zhenhao He, Runbin Shi, Cedric Renggli, Shuai Zhang, Theodoros Rekatsinas, Torsten Hoefler, et al. Co-design hardware and algorithm for vector search. *arXiv preprint arXiv:2306.11182*, 2023.
- [50] Insoon Jo, Duck-Ho Bae, Andre S Yoon, Jeong-Uk Kang, Sangyeun Cho, Daniel DG Lee, and Jaehoon Jeong. Yoursql: a high-performance database system leveraging in-storage computing. *Proceedings of the VLDB Endowment*, 9(12):924–935, 2016.
- [51] Jeff Johnson, Matthijs Douze, and Hervé Jégou. Billion-scale similarity search with gpus. *IEEE Transactions on Big Data*, 2019.
- [52] Sang-Woo Jun, Ming Liu, Sungjin Lee, Jamey Hicks, John Ankcorn, Myron King, Shuotao Xu, et al. Bluedbm: An appliance for big data analytics. In *2015 ACM/IEEE 42nd Annual International Symposium on Computer Architecture (ISCA)*, pages 1–13. IEEE, 2015.
- [53] Yangwook Kang, Yang-suk Kee, Ethan L Miller, and Chanik Park. Enabling cost-effective data processing with smart ssd. In *2013 IEEE 29th symposium on mass storage systems and technologies (MSST)*, pages 1–12. IEEE, 2013.
- [54] Sam Kaufman, Phitchaya Phothilimthana, Yanqi Zhou, Charith Mendis, Sudip Roy, Amit Sabne, and Mike Burrows. A learned performance model for tensor processing units. *Proceedings of Machine Learning and Systems*, 3:387–400, 2021.
- [55] Liu Ke, Xuan Zhang, Benjamin Lee, G Edward Suh, and Hsien-Hsin S Lee. Disaggrec: Architecting disaggregated systems for large-scale personalized recommendation. *arXiv preprint arXiv:2212.00939*, 2022.
- [56] Urvashi Khandelwal, Angela Fan, Dan Jurafsky, Luke Zettlemoyer, and Mike Lewis. Nearest neighbor machine translation. *arXiv preprint arXiv:2010.00710*, 2020.
- [57] Urvashi Khandelwal, Omer Levy, Dan Jurafsky, Luke Zettlemoyer, and Mike Lewis. Generalization through memorization: Nearest neighbor language models. *arXiv preprint arXiv:1911.00172*, 2019.
- [58] Mojtaba Komeili, Kurt Shuster, and Jason Weston. Internet-augmented dialogue generation. *arXiv preprint arXiv:2107.07566*, 2021.
- [59] Gunjae Koo, Kiran Kumar Matam, Te I, HV Krishna Giri Narra, Jing Li, Hung-Wei Tseng, Steven Swanson, and Murali Annavaram. Summarizer: trading communication with computing near storage. In *Proceedings of the 50th Annual IEEE/ACM International Symposium on Microarchitecture*, pages 219–231, 2017.
- [60] Dario Korolija, Dimitrios Koutsoukos, Kimberly Keeton, Konstantin Taranov, Dejan Milojević, and Gustavo Alonso. Farview: Disaggregated memory with operator off-loading for database engines. *arXiv preprint arXiv:2106.07102*, 2021.
- [61] Hyoukjun Kwon, Liangzhen Lai, Michael Pellauer, Tushar Krishna, Yu-Hsin Chen, and Vikas Chandra. Heterogeneous dataflow accelerators for multi-dnn workloads. In *2021 IEEE International Symposium on High-Performance Computer Architecture (HPCA)*, pages 71–83. IEEE, 2021.
- [62] Woosuk Kwon, Zhuohan Li, Siyuan Zhuang, Ying Sheng, Lianmin Zheng, Cody Hao Yu, Joseph E. Gonzalez, Hao Zhang, and Ion Stoica. Efficient memory management for large language model serving with pagedattention. In *Proceedings of the ACM SIGOPS 29th Symposium on Operating Systems Principles*, 2023.
- [63] Chris Lattner, Mehdi Amini, Uday Bondhugula, Albert Cohen, Andy Davis, Jacques Pienaar, River Riddle, Tatiana Shpeisman, Nicolas Vasilache, and Oleksandr Zinenko. Mlir: Scaling compiler infrastructure for domain specific computation. In *2021 IEEE/ACM International Symposium on Code Generation and Optimization (CGO)*, pages 2–14. IEEE, 2021.
- [64] Yejin Lee, Hyunji Choi, Sunhong Min, Hyunseung Lee, Sangwon Beak, Dawoon Jeong, Jae W Lee, and Tae Jun Ham. Anna: Specialized architecture for approximate nearest neighbor search. In *2022 IEEE International Symposium on High-Performance Computer Architecture (HPCA)*, pages 169–183. IEEE, 2022.
- [65] Charles E Leiserson. Systolic priority queues. Technical report, CARNEGIE-MELLON UNIV PITTSBURGH PA DEPT OF COMPUTER SCIENCE, 1979.
- [66] Herwig Lejsek, Friðrik Heiðar Ásmundsson, Björn Þór Jónsson, and Laurent Amsaleg. Nv-tree: An efficient disk-based index for approximate search in very large high-dimensional collections. *IEEE Transactions on Pattern Analysis and Machine Intelligence*, 31(5):869–883, 2008.
- [67] Mike Lewis, Marjan Ghazvininejad, Gargi Ghosh, Armen Aghajanyan, Sida Wang, and Luke Zettlemoyer.

- Pre-training via paraphrasing. *Advances in Neural Information Processing Systems*, 33:18470–18481, 2020.
- [68] Patrick Lewis, Ethan Perez, Aleksandra Piktus, Fabio Petroni, Vladimir Karpukhin, Naman Goyal, Heinrich Küttler, Mike Lewis, Wen-tau Yih, Tim Rocktäschel, et al. Retrieval-augmented generation for knowledge-intensive nlp tasks. *Advances in Neural Information Processing Systems*, 33:9459–9474, 2020.
 - [69] Shigang Li, Kazuki Osawa, and Torsten Hoefler. Efficient quantized sparse matrix operations on tensor cores. In *SC22: International Conference for High Performance Computing, Networking, Storage and Analysis*, pages 1–15. IEEE, 2022.
 - [70] Zhengyi Li, Cong Guo, Zhanda Zhu, Yangjie Zhou, Yuxian Qiu, Xiaotian Gao, Jingwen Leng, and Minyi Guo. Efficient activation quantization via adaptive rounding border for post-training quantization. *arXiv preprint arXiv:2208.11945*, 2022.
 - [71] Zihao Li. The dark side of chatgpt: Legal and ethical challenges from stochastic parrots and hallucination. *arXiv preprint arXiv:2304.14347*, 2023.
 - [72] Zonglin Li, Ruiqi Guo, and Sanjiv Kumar. Decoupled context processing for context augmented language modeling. *Advances in Neural Information Processing Systems*, 35:21698–21710, 2022.
 - [73] Kevin Lim, Jichuan Chang, Trevor Mudge, Parthasarathy Ranganathan, Steven K Reinhardt, and Thomas F Wenisch. Disaggregated memory for expansion and sharing in blade servers. *ACM SIGARCH computer architecture news*, 37(3):267–278, 2009.
 - [74] Kevin Lim, Yoshio Turner, Jose Renato Santos, Alvin AuYoung, Jichuan Chang, Parthasarathy Ranganathan, and Thomas F Wenisch. System-level implications of disaggregated memory. In *IEEE International Symposium on High-Performance Comp Architecture*, pages 1–12. IEEE, 2012.
 - [75] Nika Mansouri Ghiasi, Jisung Park, Harun Mustafa, Jeremie Kim, Ataberk Olgun, Arvid Gollwitzer, Damla Senol Cali, Can Firtina, Haiyu Mao, Nour Almadhoun Alserr, et al. Genstore: a high-performance in-storage processing system for genome sequence analysis. In *Proceedings of the 27th ACM International Conference on Architectural Support for Programming Languages and Operating Systems*, pages 635–654, 2022.
 - [76] Yuxian Meng, Xiaoya Li, Xiayu Zheng, Fei Wu, Xiaofei Sun, Tianwei Zhang, and Jiwei Li. Fast nearest neighbor machine translation. *arXiv preprint arXiv:2105.14528*, 2021.
 - [77] Rachit Nigam, Samuel Thomas, Zhijing Li, and Adrian Sampson. A compiler infrastructure for accelerator generators. In *Proceedings of the 26th ACM International Conference on Architectural Support for Programming Languages and Operating Systems*, pages 804–817, 2021.
 - [78] Mark Oskin, Frederic T Chong, and Timothy Sherwood. Active pages: A computation model for intelligent memory. In *Proceedings. 25th Annual International Symposium on Computer Architecture (Cat. No. 98CB36235)*, pages 192–203. IEEE, 1998.
 - [79] Myle Ott, Sergey Edunov, Alexei Baevski, Angela Fan, Sam Gross, Nathan Ng, David Grangier, and Michael Auli. fairseq: A fast, extensible toolkit for sequence modeling. *arXiv preprint arXiv:1904.01038*, 2019.
 - [80] Adam Paszke, Sam Gross, Francisco Massa, Adam Lerer, James Bradbury, Gregory Chanan, Trevor Killeen, Zeming Lin, Natalia Gimelshein, Luca Antiga, et al. Pytorch: An imperative style, high-performance deep learning library. *Advances in neural information processing systems*, 32, 2019.
 - [81] David Patterson, Thomas Anderson, Neal Cardwell, Richard Fromm, Kimberly Keeton, Christoforos Kozyrakis, Randi Thomas, and Katherine Yelick. A case for intelligent ram. *IEEE micro*, 17(2):34–44, 1997.
 - [82] Shvetank Prakash, Tim Callahan, Joseph Bushagour, Colby Banbury, Alan V Green, Pete Warden, Tim Ansell, and Vijay Janapa Reddi. Cfu playground: Full-stack open-source framework for tiny machine learning (tinyml) acceleration on fpgas. In *2023 IEEE International Symposium on Performance Analysis of Systems and Software (ISPASS)*, pages 157–167. IEEE, 2023.
 - [83] Alec Radford, Jeffrey Wu, Rewon Child, David Luan, Dario Amodei, Ilya Sutskever, et al. Language models are unsupervised multitask learners. *OpenAI blog*, 1(8):9, 2019.
 - [84] Jack W Rae, Sebastian Borgeaud, Trevor Cai, Katie Millican, Jordan Hoffmann, Francis Song, John Aslanides, Sarah Henderson, Roman Ring, Susannah Young, et al. Scaling language models: Methods, analysis & insights from training gopher. *arXiv preprint arXiv:2112.11446*, 2021.

- [85] Colin Raffel, Noam Shazeer, Adam Roberts, Katherine Lee, Sharan Narang, Michael Matena, Yanqi Zhou, Wei Li, and Peter J Liu. Exploring the limits of transfer learning with a unified text-to-text transformer. *The Journal of Machine Learning Research*, 21(1):5485–5551, 2020.
- [86] Ori Ram, Yoav Levine, Itay Dalmedigos, Dor Muhl-gay, Amnon Shashua, Kevin Leyton-Brown, and Yoav Shoham. In-context retrieval-augmented language models. *arXiv preprint arXiv:2302.00083*, 2023.
- [87] Jie Ren, Minjia Zhang, and Dong Li. Hm-ann: Efficient billion-point nearest neighbor search on heterogeneous memory. *Advances in Neural Information Processing Systems*, 33:10672–10684, 2020.
- [88] Erik Riedel, Christos Faloutsos, Garth A Gibson, and David Nagle. Active disks for large-scale data processing. *Computer*, 34(6):68–74, 2001.
- [89] Devendra Singh Sachan, Mostofa Patwary, Mohammad Shoeybi, Neel Kant, Wei Ping, William L Hamilton, and Bryan Catanzaro. End-to-end training of neural retrievers for open-domain question answering. *arXiv preprint arXiv:2101.00408*, 2021.
- [90] Sudharsan Seshadri, Mark Gahagan, Sundaram Bhaskaran, Trevor Bunker, Arup De, Yanqin Jin, Yang Liu, and Steven Swanson. Willow: A {User-Programmable}{SSD}. In *11th USENIX Symposium on Operating Systems Design and Implementation (OSDI 14)*, pages 67–80, 2014.
- [91] Yakun Sophia Shao, Jason Clemons, Rangharajan Venkatesan, Brian Zimmer, Matthew Fojtik, Nan Jiang, Ben Keller, Alicia Klinefelter, Nathaniel Pinckney, Priyanka Raina, et al. Simba: Scaling deep-learning inference with multi-chip-module-based architecture. In *Proceedings of the 52nd Annual IEEE/ACM International Symposium on Microarchitecture*, pages 14–27, 2019.
- [92] Hardik Sharma, Jongse Park, Divya Mahajan, Emmanuel Amaro, Joon Kyung Kim, Chenkai Shao, Asit Mishra, and Hadi Esmaeilzadeh. From high-level deep neural models to fpgas. In *2016 49th Annual IEEE/ACM International Symposium on Microarchitecture (MICRO)*, pages 1–12. IEEE, 2016.
- [93] Kurt Shuster, Mojtaba Komeili, Leonard Adolphs, Stephen Roller, Arthur Szlam, and Jason Weston. Language models that seek for knowledge: Modular search & generation for dialogue and prompt completion. *arXiv preprint arXiv:2203.13224*, 2022.
- [94] Gagandeep Singh, Lorenzo Chelini, Stefano Corda, Ahsan Javed Awan, Sander Stuijk, Roel Jordans, Henk Corporaal, and Albert-Jan Boonstra. Near-memory computing: Past, present, and future. *Microprocessors and Microsystems*, 71:102868, 2019.
- [95] Shaden Smith, Mostofa Patwary, Brandon Norick, Patrick LeGresley, Samyam Rajbhandari, Jared Casper, Zhun Liu, Shrimai Prabhumoye, George Zerveas, Vijay Korthikanti, et al. Using deepspeed and megatron to train megatron-turing nlg 530b, a large-scale generative language model. *arXiv preprint arXiv:2201.11990*, 2022.
- [96] Devesh Tiwari, Simona Boboila, Sudharshan Vazhkudai, Youngjae Kim, Xiaosong Ma, Peter Desnoyers, and Yan Solihin. Active flash: Towards {Energy-Efficient},{In-Situ} data analytics on {Extreme-Scale} machines. In *11th USENIX Conference on File and Storage Technologies (FAST 13)*, pages 119–132, 2013.
- [97] Ashish Vaswani, Noam Shazeer, Niki Parmar, Jakob Uszkoreit, Llion Jones, Aidan N Gomez, Łukasz Kaiser, and Illia Polosukhin. Attention is all you need. *Advances in neural information processing systems*, 30, 2017.
- [98] Xiaohui Wang, Yang Wei, Ying Xiong, Guyue Huang, Xian Qian, Yufei Ding, Mingxuan Wang, and Lei Li. Lightseq2: Accelerated training for transformer-based models on gpus. In *SC22: International Conference for High Performance Computing, Networking, Storage and Analysis*, pages 1–14. IEEE, 2022.
- [99] Zeke Wang, Hongjing Huang, Jie Zhang, and Gustavo Alonso. Shuhai: Benchmarking high bandwidth memory on fpgas. In *2020 IEEE 28th Annual International Symposium on Field-Programmable Custom Computing Machines (FCCM)*, pages 111–119. IEEE, 2020.
- [100] Laura Weidinger, John Mellor, Maribeth Rauh, Conor Griffin, Jonathan Uesato, Po-Sen Huang, Myra Cheng, Mia Glaese, Borja Balle, Atoosa Kasirzadeh, et al. Ethical and social risks of harm from language models. *arXiv preprint arXiv:2112.04359*, 2021.
- [101] Patrick Wieschollek, Oliver Wang, Alexander Sorkine-Hornung, and Hendrik Lensch. Efficient large-scale approximate nearest neighbor search on the gpu. In *Proceedings of the IEEE Conference on Computer Vision and Pattern Recognition*, pages 2027–2035, 2016.
- [102] Mark Wilkenning, Udit Gupta, Samuel Hsia, Caroline Trippel, Carole-Jean Wu, David Brooks, and Gu-Yeon Wei. Recssd: near data processing for solid state drive based recommendation inference. In *Proceedings of*

the 26th ACM International Conference on Architectural Support for Programming Languages and Operating Systems, pages 717–729, 2021.

- [103] Frank F Xu, Uri Alon, and Graham Neubig. Why do nearest neighbor language models work? *arXiv preprint arXiv:2301.02828*, 2023.
- [104] Dani Yogatama, Cyprien de Masson d’Autume, and Lingpeng Kong. Adaptive semiparametric language models. *Transactions of the Association for Computational Linguistics*, 9:362–373, 2021.
- [105] Chaoliang Zeng, Layong Luo, Qingsong Ning, Yaodong Han, Yuhang Jiang, Ding Tang, Zilong Wang, Kai Chen, and Chuanxiong Guo. {FAERY}: An {FPGA-accelerated} embedding-based retrieval system. In *16th USENIX Symposium on Operating Systems Design and Implementation (OSDI 22)*, pages 841–856, 2022.
- [106] Jialiang Zhang, Soroosh Khoram, and Jing Li. Efficient large-scale approximate nearest neighbor search on opencl fpga. In *Proceedings of the IEEE Conference on Computer Vision and Pattern Recognition*, pages 4924–4932, 2018.
- [107] Qizhen Zhang, Yifan Cai, Xinyi Chen, Sebastian Angel, Ang Chen, Vincent Liu, and Boon Thau Loo. Understanding the effect of data center resource disaggregation on production dbmss. *Proceedings of the VLDB Endowment*, 13(9), 2020.
- [108] Shijin Zhang, Zidong Du, Lei Zhang, Huiying Lan, Shaoli Liu, Ling Li, Qi Guo, Tianshi Chen, and Yunji Chen. Cambricon-x: An accelerator for sparse neural networks. In *2016 49th Annual IEEE/ACM International Symposium on Microarchitecture (MICRO)*, pages 1–12. IEEE, 2016.
- [109] Xinyi Zhang, Yawen Wu, Peipei Zhou, Xulong Tang, and Jingtong Hu. Algorithm-hardware co-design of attention mechanism on fpga devices. *ACM Transactions on Embedded Computing Systems (TECS)*, 20(5s):1–24, 2021.